

Stability of Si–C films prepared by a pulsed arc discharge method: Thermal treatment and heavy-ion irradiation

L. Khriachtchev^{a)}

Laboratory of Physical Chemistry, P.O. Box 55, FIN-00014 University of Helsinki, Finland

E. Vainonen-Ahlgren, T. Sajavaara, T. Ahlgren, and J. Keinonen

Accelerator Laboratory, P.O. Box 43, FIN-00014 University of Helsinki, Finland

(Received 29 March 2000; accepted for publication 10 May 2000)

We study Si–C films (Si content from 0 to 33 at. %) prepared with a pulsed arc discharge method. The structural modifications introduced by annealing up to 1100 °C, irradiation with 53 MeV $^{127}\text{I}^{10+}$ ions, and deposition onto heated substrates are characterized by Raman spectroscopy. For all the treatments, the structural modifications decrease when the Si concentration increases. Moreover, for high Si content (33 at. %), the energetic iodine ions are found to recover efficiently the structure degraded in preliminary high-temperature annealing. The experiments demonstrate Si-induced stabilization of the three-dimensional Si–C network, which is interpreted as deepening of the corresponding potential energy well. It is highly possible that Si–C films can possess a superior thermodynamic stability for an optimal Si concentration. © 2000 American Institute of Physics. [S0021-8979(00)02516-0]

I. INTRODUCTION

Diamond-like carbon (DLC) with various dopants (B, N, Si, etc.) is a promising material for coating technology and electronics. The incorporation of Si atoms into both hydrogenated and hydrogen-free DLC networks essentially changes their properties.^{1–6} In particular, the addition of Si can increase sp^3 fractions and reduce the size of graphitic islands.

Thermal stability of thin films is desired in many applications and reflects fundamental features of the local coordination. Annealing of DLC has repeatedly been reported to cause graphitization of the network,^{7–11} and the thermal stability increases for DLC films with a high sp^3 fraction (tetrahedral amorphous carbon).^{12,13} Growth of a DLC network on substrates heated above 200 °C leads to extensive sp^2 clusterization,¹⁴ and a similar behavior has also been observed for Si-containing DLC films prepared with a radio frequency plasma system.¹⁵ The Si incorporation has recently been found to improve thermal stability of DLC material prepared by radio frequency plasma deposition and energetic hydrocarbon beams.^{16–20}

Under irradiation with energetic heavy ions, DLC films undergo structural modifications. For instance, graphitization of high-quality DLC films exposed to 200 keV Xe^+ ions was reported by McCulloch *et al.*^{21,22} They also observed an enhancement of graphitization at elevated implantation temperatures. The irradiation of high-quality DLC with a 50 keV Ga^+ ion beam was found to decrease the graphitization temperatures in posterior annealing.²³

Raman spectroscopy has been applied extensively to characterization of silicon and carbon thin films. For DLC without dopants, Raman spectra are typically dominated by

broad scattering bands around 1560 cm^{-1} (*G* line) and 1350 cm^{-1} (*D* line) that are conventionally attributed to well-localized vibrations in sp^2 -coordinated clusters.²⁴ The low-frequency region (400–800 cm^{-1}) of the Raman scattering is believed to be due to interaction between sp^3 - and sp^2 -bonded networks.^{25,26} For Si-containing DLC, the *G* line shifts down in energy.^{3,5,19} For high Si content (≥ 50 at. %), Si–Si and C–Si bonds essentially contribute to the Raman spectra constituting broad bands around 480 and 700 cm^{-1} .¹⁸ Raman spectroscopy is useful for testing thermal stability of DLC-based films because the graphitization process can straightforwardly be characterized by employing the intensity ratio of the *D* and *G* lines.^{24,27}

In the present work, the structural stability of Si–C films prepared with a pulsed cathodic arc discharge (PCAD) method is examined by using Raman spectroscopy. In particular, we study the structural modifications introduced by energetic iodine ions for as-deposited and annealed Si–C films as a function of the Si concentration.

II. EXPERIMENT

The 500–800-nm-thick Si–C films were deposited onto crystalline Si wafers with the PCAD facilities of DIARC-Technology Inc. (Finland). The cathodes were prepared by mixing pure graphite and silicon powders that were further solidified by a hot isostatic pressing technique. Details of the deposition procedure are described elsewhere.²⁸ Annealing was performed in a quartz-tube furnace (pressure below 2×10^{-4} Pa) at temperatures from 600 to 1100 °C, the annealing time exceeding 1 h.

The time-of-flight elastic recoil detection analysis (TOF-ERDA) of elementary concentration profiles was performed with a 5 MV tandem accelerator EGP-10-II at the University of Helsinki. In the measurements, a 53 MeV beam of $^{127}\text{I}^{10+}$ was used. The detection angle was 40°, and the samples were

^{a)} Author to whom correspondence should be addressed; electronic mail: Leonid.Khriachtchev@Helsinki.Fi

tilted relatively to the beam direction by 20° . The beam electric current varied from 5 to 12 nA over an area of $\sim 6 \text{ mm}^2$, and the ion irradiation lasted from 30 to 60 min. The elementary concentrations were calculated with known geometry and by employing the Ziegler–Biersack–Littmark stopping powers for energy loss estimates.^{29,30} The film areas used in the TOF-ERDA measurements are later referred to as samples irradiated with iodine ions. The analysis of surface morphology was performed with a Zeiss 962 digital scanning electron microscope equipped with an energy dispersive x-ray detector.

The Raman spectra were recorded in the $100\text{--}2800 \text{ cm}^{-1}$ region by using a single-stage spectrometer (Acton SpectralPro 500I) in a low-resolution mode ($\sim 10 \text{ cm}^{-1}$) equipped with a 1024×256 pixel charge coupled device (CCD) camera (Andor InstaSpec IV). The 514.5 nm radiation of an Ar^+ laser (Omnichrome 543-AP) was directed to a sample at $\sim 45^\circ$ in P polarization and focused to a $\sim 50 \mu\text{m}$ spot, the laser power being $\sim 50 \text{ mW}$. The Raman scattering light was transmitted to the spectrometer through a collecting optic, a holographic filter (Kaiser Super-Notch-Plus), and an optical fiber.

In order to characterize the Raman spectra numerically, conventional two-Gaussian decomposition of the dominating spectral feature to *D* and *G* lines with a suitable background is used, which provides information of sp^2 clusterization.^{24,27} In addition, we analyze the Raman intensity ratio $R = I_{500}/I_{1550}$ and the slope $S = (I_{1300} - I_{1100})/I_{1100}$ correlating with a sp^3 fraction η of DLC.^{31,32} The band positions are shifted for Si-containing DLC. Therefore, we consider in the present article the generalized *R* parameter where I_{1550} denotes the maximum intensity of the dominating spectral feature in the higher-frequency ($1400\text{--}1600 \text{ cm}^{-1}$) spectral region.

III. EXPERIMENTAL RESULTS

A. Film composition

The TOF-ERDA measurements suggested that Si atoms were evenly distributed throughout the films and no loss of Si occurred during annealing up to 1100°C . The concentrations of Si were measured to be 0, 6, 15, and 33 at. % for four sets of the samples. For the purpose of another study, the samples contained some amount of deuterium that increased with the Si concentration from 2.9 at. % (no Si) to 4.8 at. % (33 at. % Si). The amounts of O and H impurities increased with the Si concentration from 0.1 at. % (no Si) up to 1–2 at. % (33 at. % Si). An upper limit of 0.1 at. % was estimated for other contamination like Fe and Ni originating from the deposition equipment. Under annealing, the H and D concentrations decreased in the film bulk and a diffusion-like behavior was observed in the surface region.³³

The scanning electron microscopy measurements indicated the presence of microparticles at the film surface, and the average size was the smallest ($0.3 \mu\text{m}$) for the Si-free films and the largest ($3 \mu\text{m}$) for Si content of 6 at. %. The observed microparticles were most probably extracted by the arc discharge from the cathode material.

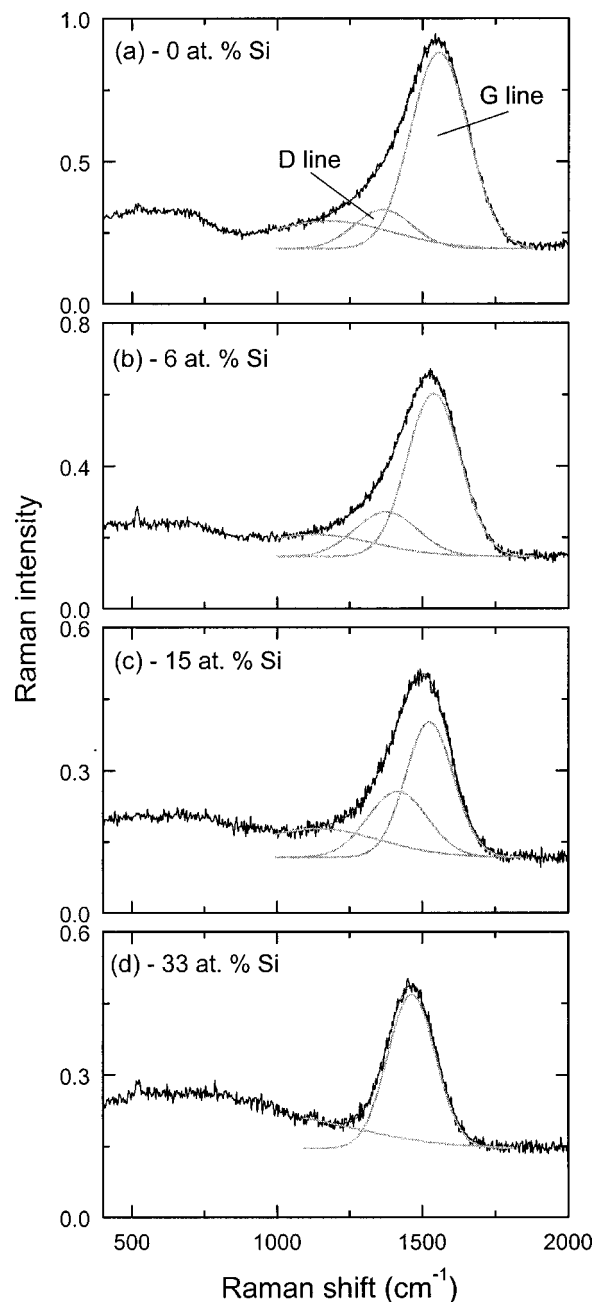


FIG. 1. Raman spectra of Si–C films as deposited at 20°C . The Si concentrations (0, 6, 15, and 33 at. %) are given in the plots, and the conventional decomposition of the dominating feature to the *D* and *G* lines is shown. In plot (d), the *D* and *G* lines coincide.

B. Raman spectra

Figure 1 presents the Raman spectra of the Si–C films deposited onto room-temperature substrates. The corresponding Raman parameters versus the Si concentration are given by solid squares in Fig. 2. The Raman spectra of the Si-free DLC films show a *D/G* ratio of 0.2, *G*-line position at 1560 cm^{-1} , *D*-line position at 1350 cm^{-1} , $R = 0.35$, and $S = 0.4$. When the Si concentration increases, the *G* line shifts down and *D* line up in energy, and they coincide at $\sim 1460 \text{ cm}^{-1}$ for the highest Si content (33 at. %). In addition, both the *D/G* ratio and the generalized *R* parameter increase with the Si concentration.

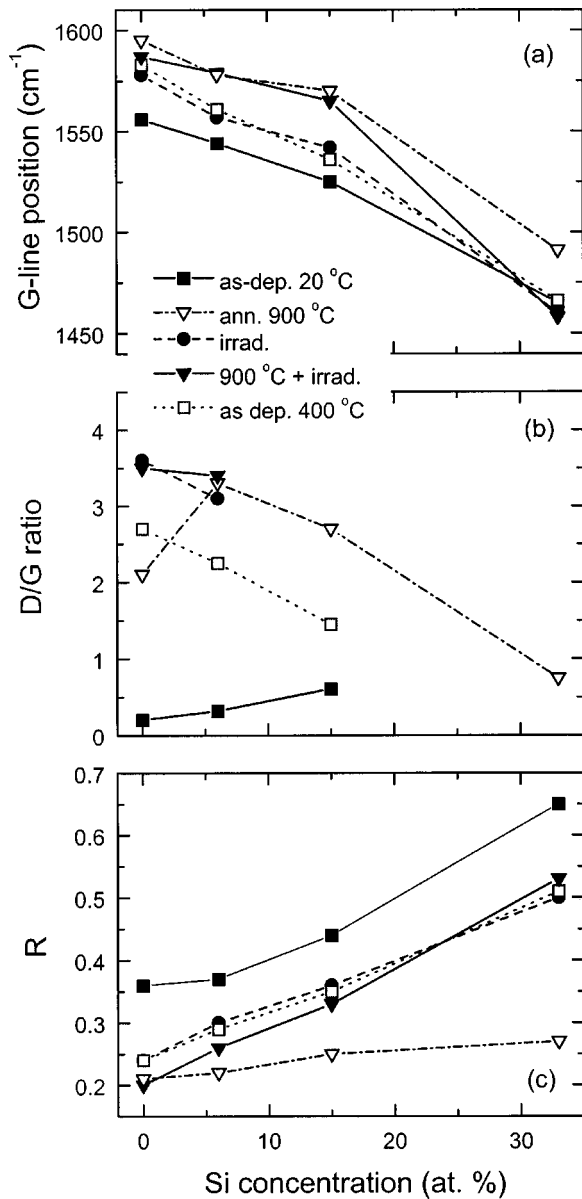


FIG. 2. Raman parameters of Si-C films as a function of the Si concentration. The data are presented for the following films: as deposited at 20 °C (solid squares), annealed at 900 °C (open triangles), irradiated with iodine ions (solid circles), annealed at 900 °C and afterwards irradiated with iodine ions (solid triangles), and as deposited at 400 °C (open squares). For some of the samples, the D/G ratios cannot be reliably obtained, and they are not reported. The annealed and irradiated films were deposited at 20 °C.

The Raman parameters of the films deposited at 400 °C as a function of the Si concentration are shown in Fig. 2 (open squares). The Si-free carbon material grown at the elevated temperature is essentially sp^2 coordinated as evidenced by $R=0.24$,^{31,32} and the sp^2 clusterization is rather extensive because the G line is shifted up to 1583 cm^{-1} and the D/G ratio is as large as 2.7.²⁷ When Si is added, the D/G ratio decreases, whereas the R parameter and G -line position behave similarly in the case of room-temperature deposition. For the highest Si content (33 at. %), the Raman spectra of the films deposited at 400 °C and at room temperature are very similar although the R parameter is still somewhat smaller for the higher-temperature deposition.

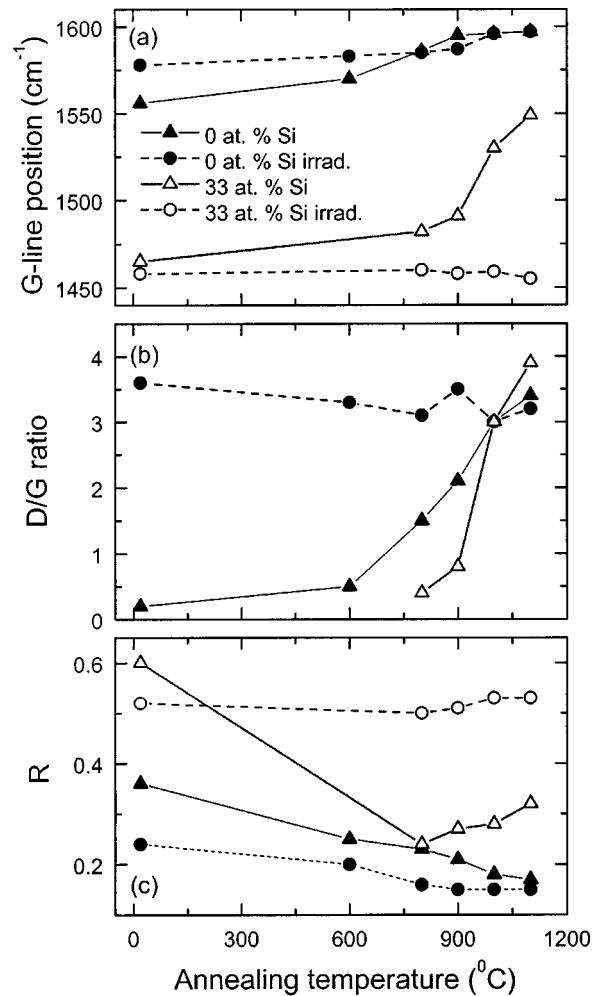


FIG. 3. Raman parameters of Si-C films with Si contents of 0 and 33 at. % as a function of the annealing temperature. The data for as-deposited (triangles) and ion-irradiated (circles) films are presented. The ion irradiation was performed after annealing. For some of the samples, the D/G ratios cannot be reliably obtained, and they are not reported. The samples were deposited at 20 °C.

The effect of annealing at 900 °C as a function of the Si concentration is presented in Fig. 2 (open triangles). It is seen that the annealing shifts the G lines up in energy, decreases the R parameters, and increases the D/G ratio. The Si-concentration dependence of the Raman parameters for ion irradiation (solid circles) closely follows the behavior obtained in the 400 °C deposition. When the ion irradiation is carried out after annealing at 900 °C (solid triangles), no additional effect is seen for low Si content and clear recovery of the as-deposited structure occurs for the highest Si concentration.

Figure 3 presents the Raman parameters of the films with Si concentrations of 0 and 33 at. % as a function of the annealing temperature. For the Si-free films without ion irradiation (solid triangles), the spectra display progressive graphitization when the annealing temperature increases as suggested by upshifting G lines and increasing D/G ratios,^{24,27} and the R parameter decreases indicating a reduction of the sp^3 fraction.^{31,32} For the highly Si-doped material (open triangles), the G -line position is quite stable in anneal-

ing at 800 and 900 °C and changes considerably at temperatures ≥ 1000 °C, but the efficient decrease of R occurs already at 600 °C.

Irradiation with high-energy iodine ions leads to graphitization of the Si-free DLC films (solid circles in Fig. 3). For the highest Si content (33 at. %), the irradiation with iodine ions results in Raman spectra which are very close to those of the as-deposited films, and the preliminary annealing has a minor effect on the resulting structure (open circles). For intermediate Si content (15 at. %), the ions produce quite a broad Raman band without well-defined G and D lines so that the extraction of their parameters is not reliable, nevertheless, the structure after ion irradiation is also quite independent of preliminary annealing.

As a final experimental observation, we found no evidence of small Si crystallites in the as-deposited and treated samples. Small Si crystallites should be easily observable by a Raman scattering band in the 510–520 cm^{-1} region.³⁴ Weak peaks at ~ 520 cm^{-1} appearing occasionally in our spectra are rather applicable to the Si crystalline substrates because they do not show a systematic dependence on the Si concentration. The Raman spectrum of a Si-doped film on an Al substrate displays no Si crystallites hence supporting this conclusion. We observed no Si crystallites rising in annealing, which suggests the absence of extensive diffusion and clusterization of Si atoms in annealing up to 1100 °C. On the other hand, amorphous Si grains are more difficult to detect in Si–C films because the corresponding phonon band is very broad. Amorphous Si structures can crystallize at about 1100 °C even if their size is below 2 nm.^{35,36} Zaharias *et al.* reported crystallization of 3-nm-thick Si amorphous layers at 1100 °C and crystallization of 5 nm layers below 1050 °C.³⁷ These data give the upper limit of sizes for amorphous Si grains that are possible in essential amounts in our films. It is worth mentioning that heavy-ion treatment of crystalline Si leads rather to amorphization of the network.³⁸

IV. DISCUSSION

For the Si-free DLC films deposited at room temperature, the measured R and S parameters yield $\eta \sim 45\%$.^{31,32} This sp^3 fraction seems to be a typical value for DLC films prepared by using a PCAD method with a straight solenoid. The averaged sp^3 fraction is possibly influenced by the presence of large sp^2 -bonded clusters, and the network between the clusters might possess a higher sp^3 fraction. The extensive sp^2 -coordinated structures are probably responsible for relatively large absorption of PCAD DLC when compared with DLC of a similar sp^3 fraction and prepared with mass-separated ion beams.³⁹ Similarly, the present Si-free DLC material possesses a quite large absorption coefficient of $\geq 5 \times 10^4$ cm^{-1} as estimated at 514 nm.

For Si-doped DLC, the shifts of the G lines down in energy have conventionally been attributed to the influence of Si–C bonds on the vibrations of sp^2 -coordinated carbon clusters. The present study shows that the D lines are also changed by the Si incorporation, shifting up in energy for higher Si content. It is plausible that Si atoms can link sp^2 -bonded carbon clusters in a Si–C network, as

sp^3 -bonded C atoms are described to do in a model of DLC.²⁴ In addition, Si atoms might incorporate into the sp^2 -bonded plane clusters changing their symmetry and probably establishing bonds with external atoms. The E_{2g2} and disorder modes are introduced for pure sp^2 -bonded carbon clusters,²⁴ and incorporation of Si atoms changes the vibrational density of states. Nevertheless, the analogies of the E_{2g2} and disorder modes seem to be degenerate for the highest Si content (33 at. %). The vibrational analysis of pure silicon (Ref. 40) and carbon (Refs. 25 and 26) lattices is known, but no detailed consideration of a mixed Si–C network is available.

We observed an increase of the D/G ratio from 0.2 for the Si-free films to 0.6 for the Si concentration of 15 at. %. This trend clearly disagrees with that reported by Wu and Hon who observed a decrease of the D/G ratio from 1.25 to 0.9 when the Si concentration increased from 0 to 13 at. %.¹⁵ This opposite behavior can be explained by assuming a poorer diamond-like quality of their Si-free DLC films, probably possessing large sp^2 -bonded clusters. For DLC, the D/G ratio is known to measure the sp^2 cluster size,^{24,27} and D lines are practically absent in the best DLC films with $\eta \sim 80\%$.^{41,42} In our Si-free films, sp^2 clusterization is not extensive, and the incorporation of small amounts of Si increases sp^2 -coordinated clusters, which is reflected in an increase of the D/G ratio and possibly corresponds to the documented impurity-enhanced sp^2 clusterization.⁴³ It is worth noting that the correlation between the size of sp^2 -bonded clusters and the D/G ratio was found for DLC without dopants,²⁷ and it can be numerically different in the present case of Si-containing DLC films.

It should be emphasized that the observed increase of D/G ratios with the Si concentration does not contradict the literature reports on an increase of a sp^3 fraction while doping DLC with Si. Indeed, D/G ratios measure rather the size of sp^2 -coordinated cluster than the sp^3 fraction. Moreover, it is seen in Fig. 2(c) that the generalized R parameter increases with the Si concentration. The low-frequency vibrations (around 500 cm^{-1}) are known to be enhanced in sp^3 -rich DLC,^{31,32,41} and $R=0.65$ measured for the highest Si concentration yields $\eta \sim 80\%$, in good agreement with the literature data on similar Si-containing materials.¹⁹ Of course, the $\eta(R)$ function was established for Si-free DLC,^{31,32} therefore, this agreement should be considered with caution. Nevertheless, the correspondence is remarkable.

The annealing-induced modifications of Raman spectra observed for the Si-free DLC films seem to correspond to those reported by Kalish *et al.* for $\eta \sim 40\%$,¹³ which resembles our experimental conditions. Unfortunately, Kalish *et al.* employed the Breit–Wigner–Fano line shape in the fitting procedure, which is not conventional and hence complicates the comparison of the results. In particular, they have reported G lines shifting in annealing up to 1620 cm^{-1} , i.e., well above the value of graphite, which is difficult to comment. Graphitization of our Si-free DLC films occurs at higher annealing temperatures than were observed in Refs. 16, 19, and 20. The differences in graphitization temperatures should be connected with diamond-like quality of the material, as suggested in Ref. 13.

For the annealed Si-containing DLC films, decomposition of sp^3 C–C bonds and growth of graphite-like structures take place, which is indicated by a decrease of R and an increase of the G -line frequency and D/G ratio. A small increase of R , observed in the higher-temperature region for the 33 at. % Si samples, might reflect formation of Si–C and Si–Si bonds and destruction of C–C bonds when Si atoms incorporate into carbon aromatic rings. The behavior seen by us in annealing corresponds qualitatively to the known literature data.^{16,17,19,20} However, the structural modification observed in the present study occurs at somewhat higher temperatures, which most probably originates from differences in the deposition methods.

The relatively low G -line frequency measured after annealing of Si–C films with respect to that of graphite was used as an indicator of the minor graphitization in Refs. 19 and 20. This concept deserves a comment. For a Si–C material, the G lines can be rather low in energy even when the three-dimensional network collapses in favor of a quasiplanar structure. In this situation, the planar complexes contain both C and Si atoms, and their vibrations are different from those of pure graphite. To support this idea qualitatively, we refer to very different vibrational properties of benzene and silabenzene.⁴⁴ Thus, the fact that the G -line position does not coincide exactly with that of graphite does not mean stability of the three-dimensional Si–C structure because the aromatic rings incorporated with Si atoms can dominate. It is difficult to expect numerous unperturbed carbon clusters to exist when the material contains Si atoms in considerable amounts. We suppose that the quasiplanar structures formed in annealing of a Si–C material are essentially doped with Si atoms. In addition, small odd-membered Si rings have been found to be stable,⁴⁵ and they are intuitively possible in the annealed material. The shift of the G lines up in energy observed in annealing of the Si–C films might indicate a temperature-induced destruction of inter-cluster links by fourfold Si atoms. On the other hand, the partial Si-introduced stabilization under annealing is indicated in our spectra by the delayed increase of the D/G ratio, as seen in Fig. 3(b). In fact, annealing at 900 °C strongly changes the Raman spectra of the Si-free DLC films, whereas the modification is smaller for the highest Si content (33 at. %).

Our experiments with deposition at 400 °C and with iodine-ion irradiation demonstrate more clearly the stabilization effect. For the highest Si content, these two treatments produce a minor effect in the Raman spectra when compared with the material as deposited at room temperature (see Fig. 2). The observed stabilization of the three-dimensional Si–C network should be connected with Si-induced deepening of the potential energy well.

Most interestingly, the exposure to 53 MeV iodine ions recovers the highly Si-doped structure degraded in the preliminary annealing. This recovery suggests the similarity in energy dissipation during milling of the Si–C network with energetic particles and during the deposition process. The growth of a dense DLC network is conventionally considered to occur in the film bulk where energetic carbon ions are capable of penetrating, which is referred to as the subplantation model.^{46,47} The relevant discussions on energy relax-

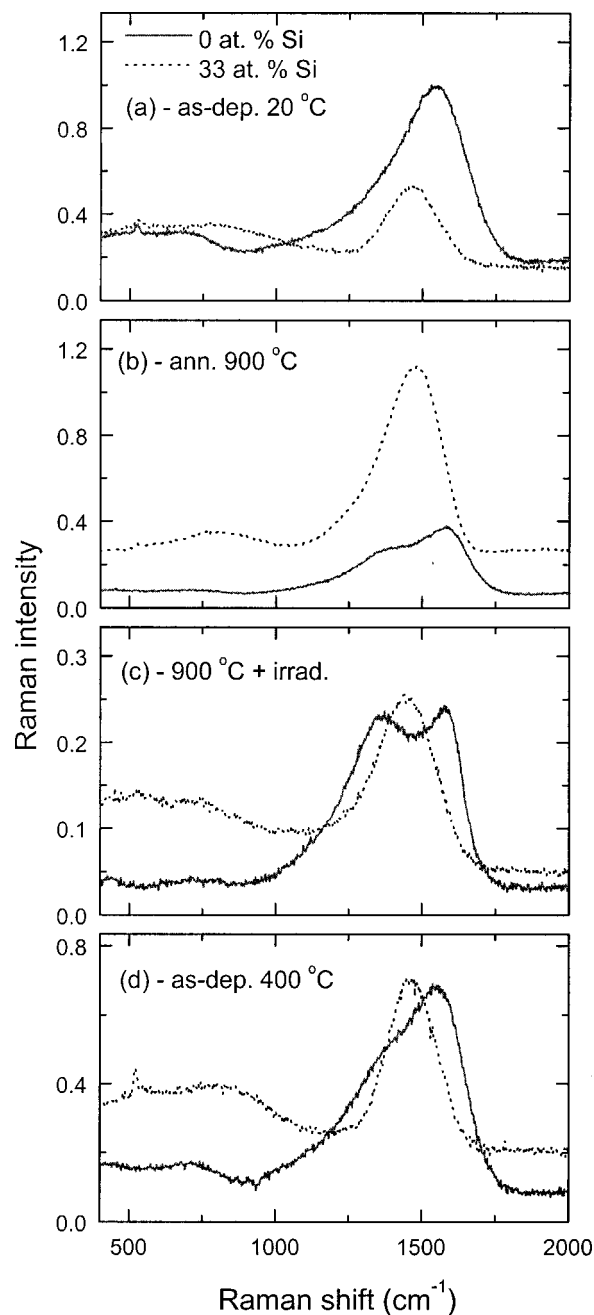


FIG. 4. Raman spectra of Si–C films with Si concentrations of 0 and 33 at. %. The following films are presented: (a) as deposited at 20 °C, (b) annealed at 900 °C, (c) irradiated with iodine ions (after annealing at 900 °C), and (d) as deposited at 400 °C. The annealed and irradiated films were deposited at 20 °C. The figure highlights the thermodynamic stabilization of the Si–C network.

ation during ion-assisted growth of DLC can be found elsewhere.⁴⁸ One can see essential qualitative analogies between the energy-redistribution processes during film growth and posterior heavy-ion irradiation although the involved ion energies are very different, indeed. On the other hand, the energy transfer in the higher-energy process is spatially delocalized hence decreasing the numerical difference in relaxation at various excitation energies.

By using the SRIM code,²⁹ we modeled energy transfer during a collision cascade produced by a 53 MeV iodine atom in a Si–C lattice. The travel distance of the 53 MeV

iodine ion in a Si–C network was estimated to be $\sim 7 \mu\text{m}$ exceeding the film thickness and hence suggesting a depth-homogeneous milling process, which distinguishes the present case from conventional implantation (see, for example, Refs. 21–23). An averaged energy transfer per one displacement was estimated to be 130 eV, and this value does not exceed by much the ion energy (~ 100 eV) used in the deposition procedure. In accord with these estimates, the experimental data presented in Fig. 2 suggest that the process of ion irradiation is somewhat more energetic than that during deposition at room temperature but rather resembles deposition at 400°C .

Ion irradiation of the Si-free DLC films did not reproduce the as-deposited structure indicating a shallow potential well of atoms in the three-dimensional metastable configuration. This observation qualitatively corresponds to the known fact that a sp^3 fraction of DLC without dopants decreases at high deposition energy^{41,42} and under heavy-ion bombardment.^{21–23} In contrast with Si-free DLC, the resulting potential well of the three-dimensional structure with the highest Si content (33 at. %) is deep enough to trap the system during the high-energy relaxation process. For the intermediate Si concentration of 15 at. %, the system relaxes under ion irradiation to a more distorted network, which is reflected by the broad Raman bands and indicates a more shallow potential energy minimum when compared with the higher Si concentration. Nevertheless, some recovery of the annealed films with the intermediate Si concentration is produced by iodine ions as well.

Finally, the dependence of the stabilization effect on the Si concentration should be emphasized. The stabilization effect is practically absent for lower Si contents (6 at. %), and it increases with the Si concentration. The lattice stability probably correlates with the depth of the potential energy well trapping the metastable Si–C structures, and it should have an energetic optimum versus the relative concentration. Such an optimal structure might be rather sensitive to the elementary composition with respect to a barrier for graphitization. We suggest that the optimal three-dimensional Si–C configuration might occupy a quasiglobal minimum of the potential energy surface, which qualitatively distinguishes it from pure carbon networks with a global energy minimum at the two-dimensional configuration. It can be interpreted that the mismatch between Si and C networks establishes thermodynamic stability of the three-dimensional Si–C amorphous structure. An experimental and theoretical search for an energetically optimized Si–C structure seems to be an attractive study. In addition, it is interesting to experimentally study the related processes when adding Si to DLC of a higher quality. The thermodynamic stability of such high-quality Si–C material might exceed that of tetrahedral amorphous carbon.

V. CONCLUSIONS

We have studied structural modifications of Si–C films prepared by a PCAD method in thermal treatment and under heavy-ion irradiation. The essential observations are demonstrated by the Raman spectra presented in Fig. 4:

(a) For the films deposited at room temperature, the Si incorporation into sp^2 -bonded C clusters changes their vibrations, and the conventional *G* and *D* lines coincides with each other at $\sim 1460 \text{ cm}^{-1}$ for the Si concentration of 33 at. %. The ratio between intensities at low and high frequencies increases with the Si concentration, probably reflecting the increase of the sp^3 fraction similar to the dependence known for Si-free DLC films.^{31,32}

(b) The Si incorporation decreases to some extent graphitization of the material in annealing. An extensive graphitization process is observed for the Si-free DLC films at 900°C but the graphitization is quite minor when the Si concentration is 33 at. %. In annealing at 1000 – 1100°C , the Si–C three-dimensional structure collapses to pseudographite that can probably be described as an essentially planar carbon structure containing Si atoms.

(c) The Si–C network is stable under exposure to very energetic iodine ions. For the Si concentration of 33 at. %, the result of ion irradiation is essentially independent of preliminary annealing. This observation introduces the recovery of thermally collapsed structure by the ion milling. We suggest that the energy-relaxation processes are qualitatively similar under the high-energy ion irradiation and during the film growth.

(d) The incorporation of Si decreases graphitization when the material is deposited onto a heated substrate (400°C). This observation further highlights a deepening of the potential energy well of the three-dimensional Si–C structure at a specific relative concentration. It is highly possible that the Si–C network can possess a superior thermodynamic stability for an optimal Si concentration.

ACKNOWLEDGMENTS

This work was supported in part by the Academy of Finland (Project No. 46798) and by the Association Euratom-TEKES. The authors thank J. Kolehmainen and J. Partanen (DIARC-Technology Inc.) for providing the samples. The electron microscope unit of the University of Helsinki is acknowledged for putting the scanning electron microscope at our disposal.

- ¹J. Bullo and M. P. Schmidt, *Phys. Status Solidi B* **143**, 345 (1987).
- ²F. Demichelis, C. F. Pirri, and A. Tagliaferro, *Mater. Sci. Eng., B* **11**, 313 (1992).
- ³C. D. Martino, F. Demichelis, and A. Tagliaferro, *Diamond Relat. Mater.* **3**, 547 (1994).
- ⁴K.-R. Lee, M.-G. Kim, S.-J. Cho, K. J. Eun, and T.-Y. Seong, *Thin Solid Films* **308**–**309**, 263 (1997).
- ⁵M. Balden, J. Roth, and C. H. Wu, *J. Nucl. Mater.* **258**–**263**, 740 (1998).
- ⁶S. Lee, D.-S. Kim, S.-G. Rhee, S.-G. Oh, and K.-R. Lee, *Thin Solid Films* **341**, 68 (1999).
- ⁷M. P. Nadler, T. M. Danovan, and A. K. Green, *Thin Solid Films* **116**, 241 (1984).
- ⁸J. Wagner, M. Ramsteiner, C. Wild, and P. Koidl, *Phys. Rev. B* **40**, 1817 (1989).
- ⁹J. Robertson, *Prog. Solid State Chem.* **21**, 199 (1991).
- ¹⁰J. C. Knight, T. F. Page, and H. W. Chandler, *Surf. Coat. Technol.* **49**, 519 (1991).
- ¹¹D. R. Tallant, J. E. Parmeter, M. P. Siegel, and R. L. Simpson, *Diamond Relat. Mater.* **4**, 191 (1995).
- ¹²S. Anders, J. Diaz, J. W. Ager III, R. Yu Lo, and D. B. Bogy, *Appl. Phys. Lett.* **71**, 3367 (1997).

- ¹³R. Kalish, Y. Lifshitz, K. Nugent, and S. Praver, *Appl. Phys. Lett.* **74**, 2936 (1999).
- ¹⁴B. K. Tay, X. Shi, E. J. Lui, H. S. Tan, and L. K. Cheah, *Thin Solid Films* **346**, 155 (1999), and references therein.
- ¹⁵W.-J. Wu and M.-H. Hon, *Thin Solid Films* **345**, 200 (1999).
- ¹⁶W.-J. Wu and M.-H. Hon, *Surf. Coat. Technol.* **111**, 134 (1999).
- ¹⁷S. S. Camargo, Jr., R. A. Santos, A. L. Baia Neto, R. Carius, and F. Finger, *Thin Solid Films* **332**, 130 (1998).
- ¹⁸A. L. Baia Neto, S. S. Camargo, Jr., R. Carius, F. Finger, and W. Beyer, *Surf. Coat. Technol.* **120,121**, 395 (1999).
- ¹⁹H. Huck, E. B. Halac, C. Oviedo, G. Zampieri, R. G. Pregliasco, E. V. Alonso, M. E. Reinoso, and M. A. R. de Benyacar, *Appl. Surf. Sci.* **141**, 141 (1999).
- ²⁰E. B. Halac, H. Huck, C. Oviedo, M. E. Reinoso, and M. A. R. de Benyacar, *Surf. Coat. Technol.* **122**, 51 (1999).
- ²¹D. G. McCulloch, E. G. Gerstner, D. R. McKenzie, S. Praver, and R. Kalish, *Phys. Rev. B* **52**, 850 (1995).
- ²²D. G. McCulloch, D. R. McKenzie, S. Praver, A. R. Merchant, E. G. Gerstner, and R. Kalish, *Diamond Relat. Mater.* **6**, 1622 (1997).
- ²³A. Stanishevsky and L. Khriachtchev, *J. Appl. Phys.* **86**, 7052 (1999).
- ²⁴M. Yoshikawa, *Mater. Sci. Forum* **52,53**, 365 (1989).
- ²⁵C. Z. Wang and K. M. Ho, *Phys. Rev. Lett.* **71**, 1184 (1993).
- ²⁶D. A. Drabold, P. A. Fedders, and P. Stumm, *Phys. Rev. B* **49**, 16 415 (1994).
- ²⁷D. G. McCulloch, S. Praver, and A. Hoffman, *Phys. Rev. B* **50**, 5905 (1994).
- ²⁸E. Vainonen, J. Likonen, T. Ahlgren, P. Haussalo, J. Keinonen, and C. H. Wu, *J. Appl. Phys.* **82**, 3791 (1997).
- ²⁹J. F. Ziegler, SRIM-98 computer code (private communication); J. F. Ziegler, J. P. Biersack, and U. Littmark, *The Stopping and Range of Ions in Solids* (Pergamon, New York, 1985).
- ³⁰J. Jokinen, J. Keinonen, P. Tikkanen, A. Kuronen, T. Ahlgren, and K. Nordlund, *Nucl. Instrum. Methods Phys. Res. B* **119**, 533 (1996).
- ³¹L. Khriachtchev, R. Lappalainen, M. Hakovirta, and M. Räsänen, *Diamond Relat. Mater.* **6**, 694 (1997).
- ³²A. Stanishevsky, L. Khriachtchev, R. Lappalainen, and M. Räsänen, *Diamond Relat. Mater.* **6**, 1026 (1997).
- ³³E. Vainonen-Ahlgren (unpublished).
- ³⁴Ch. Ossadnik, S. Veprek, and I. Gregora, *Thin Solid Films* **337**, 148 (1999), and references therein.
- ³⁵P. D. Persans, A. Ruppert, and B. Abeles, *J. Non-Cryst. Solids* **102**, 130 (1988).
- ³⁶L. Khriachtchev, M. Räsänen, S. Novikov, O. Kilpelä, and J. Sinkkonen, *J. Appl. Phys.* **86**, 5601 (1999).
- ³⁷M. Zaharias, J. Bläsing, P. Veit, L. Tsybeskov, K. Hirschman, and P. M. Fauchet, *Appl. Phys. Lett.* **74**, 2614 (1999).
- ³⁸S. Dey, C. Roy, A. Pradham, and S. Varma, *J. Appl. Phys.* **87**, 1110 (2000).
- ³⁹L. Khriachtchev, R. Lappalainen, and M. Räsänen, *Thin Solid Films* **325**, 192 (1998).
- ⁴⁰N. Maley, D. Beeman, and J. S. Lannin, *Phys. Rev. B* **38**, 10 611 (1988).
- ⁴¹L. Khriachtchev, M. Hakovirta, R. Lappalainen, and M. Räsänen, *Phys. Lett. A* **217**, 354 (1996).
- ⁴²S. Praver, K. W. Nugent, Y. Lifshitz, G. D. Lempert, E. Grossman, J. Kulik, I. Avigal, and R. Kalish, *Diamond Relat. Mater.* **5**, 433 (1996).
- ⁴³L. Khriachtchev, M. Räsänen, and R. Lappalainen, *J. Appl. Phys.* **82**, 413 (1997).
- ⁴⁴G. Maier, G. Mihm, R. O. W. Baumgartner, and H. P. Reisenauer, *Chem. Ber.* **117**, 2337 (1984).
- ⁴⁵P. Melinon, P. Keghelian, B. Prevel, A. Perez, G. Guiraud, J. LeBrusq, J. Lerme, M. Pellarin, and M. Broyer, *J. Chem. Phys.* **107**, 10 278 (1997).
- ⁴⁶Y. Lifshitz, S. R. Kasi, and J. W. Rabalais, *Phys. Rev. Lett.* **62**, 1290 (1989).
- ⁴⁷J. Robertson, *Diamond Relat. Mater.* **3**, 361 (1994).
- ⁴⁸F. Rossi, *Chaos* **10**, 2019 (1999), and references therein.